PERGAMON

Deep-Sea Research II 49 (2002) 3513–3528

DEEP-SEA RESEARCH
PART II

www.elsevier.com/locate/dsr2

Penetration of solar radiation into the water column of the central subtropical Atlantic Ocean—optical properties and possible biological consequences

H. Piazena[a,*], E. Perez-Rodrigues[b], D.-P. Häder[a], F. Lopez-Figueroa[b]

[a] *Friedrich-Alexander Universität, Institut für Botanik und Pharmazeutische Biologie, Staudtstr. 5, D-91058 Erlangen, Germany*
[b] *Departamento de Ecologia, Facultad de Ciencias, Universidad de Malaga, Campus Universitario de Teatinos s/n, E-29071 Malaga, Spain*

Received 5 September 2000; received in revised form 10 January 2001; accepted 20 January 2001

Abstract

The optical properties of the waters as well as the penetration of both solar ultraviolet radiation (UVR) and photosynthetically active radiation (PAR) were analyzed at different stations of the central subtropical Atlantic Ocean during the AZORES II cruise of the research vessel "Hesperides" in April 1999 to assess the impact of solar UVR on microorganisms populating highly transparent oceanic waters. The investigation was based on direct spectral measurements of the scalar and downward-solar irradiance between 290 and 750 nm at different depths using a temperature-stabilized double monochromator spectroradiometer (Optronic, type 754) with a highly sensitive 4π sensor connected to the entrance slit by a 20-m quartz fiber cable. In addition, the Secchi depth was measured, and water samples of different depths at each station were analyzed to determine the concentration and optical properties of phytoplankton as well as attenuating substances such as seston and gelbstoff in the column. Using the spectral irradiance data at different depths as well as the vertical irradiance profiles at different wavelengths, the following parameters were calculated: the spectral attenuation coefficients, the spectral depths of penetration to 1% of the sub-surface value ("1% depths"), the 1% depths for the ranges UV-B, UV-A and PAR, as well as the water type in the Jerlov system of optical classification. The optical properties of the waters investigated can be classified into the oceanic types OI–OII in the Jerlov system, which are characterized by very small concentrations of seston and of gelbstoff, which are the main absorbers for UV radiation in natural waters. The Secchi depths varied between about 15 m (type OII) to about 45 m (type OI) showing ratios to the 1% depths of PAR of about 0.21 to about 0.31. Values of the same order were found for the depths of the maximal concentration of chlorophyll *a*, which varied between 45 and 100 m during midnight and between 70 and 110 m during noon, showing also significant increases with increasing transparency of the waters. In contrast, the 1% depths for the penetration of solar UV irradiance were found between 12 and 19 m (type OII) and between 26 and 31 m (type OI) for UV-B whereas their values ranged for UV-A between 29 and 65 m (type OII) and between 55 and 93 m (type OI). Thus, solar UV-B penetrates up to about 25% of the photic zone in these waters whereas for UV-A about 75–93% were found. So, solar UVR may significantly affect both the photosynthetic activity by photoinhibition as well as the composition of the kind of species populating different depths of the column by further effects such as DNA damage and inhibition of motility. The role of UVR as a selection factor is shown by a strong absorption peak in the UV range of the water samples, which occurred only when the organisms

*Corresponding author. Present address: Humboldt-Universität, Klinik und Poliklinik für Hautkrankheiten (Charité), Schumannstr. 20/21, D-10117 Berlin, Germany. Tel.: +49-9131-8528216; fax: +49-9131-8528215.

E-mail addresses: helmut.piazena@charite.de (H. Piazena), eduperez@uma.es (E. Perez-Rodrigues), dphaeder@biologie.uni-erlangen.de (D.-P. Häder), felix_lopez@uma.es (F. Lopez-Figueroa).

0967-0645/02/$ - see front matter
PII: S0967-0645(02)00093-0

were sampled in the near-surface layer indicating different species composition with depth.

1. Introduction

The penetration of solar ultraviolet radiation (UVR) and photosynthetically active radiation (PAR) into natural waters strongly depends on wavelength as well as on the concentration and composition of attenuating substances such as seston and gelbstoff. In the Jerlov system of optical classification, marine waters (Jerlov, 1970, 1976; Hoerslev, 1986) are divided into five oceanic (OI, OIa, OIb, OII, OIII) and nine coastal water types (C1–C9). The system was extended by the types C10–C20 to characterize the optical properties of more turbid coastal waters (Piazena and Häder, 1997). Type OI characterizes the optical properties of natural waters, with the highest transparency (Smith and Baker, 1978, 1981) showing depths of penetration to 1% of the subsurface solar irradiance of about 31 m for UV-B (280–315 nm), of about 120 m for UV-A (315–400 nm) and of about 170 m for PAR. The penetration of solar radiation into the water column decreases with increasing water type. For instance, for water type C15, which is found in a highly turbid inner lagoon of the Baltic Sea with little water exchange, the 1% depths of penetration range on the order of 0.5 m for UV-B, of about 1 m for UV-A and of about 5 m for PAR (Piazena and Häder, 1994, 1997).

Phytoplankton, which is the basis of the aquatic food webs as well as one of the most important sinks of atmospheric carbon dioxide by photosynthesis and biomass production (Häder et al., 1994), uses various mechanisms of orientation and vertical migration to optimize the received fluence rate of photosynthetically effective solar radiation, which decreases with depth and depends on both the incident irradiance and on the optical properties of the water (Häder and Reinecke, 1991).

However, solar radiation not only stimulates photosynthesis. High fluence rates in the UV and PAR range may cause photoinhibition of the photosynthetic system; in addition, exposure to high doses of UVR may result in molecular and cellular damages such as chlorophyll bleaching, changes of the DNA structure, damages to membranes, proteins and pigments as well as in functional disturbances of the organisms such as inhibition of motility and of the photo- or gravitactic orientation (Booth et al., 1997; Wängberg and Selmer, 1997; Vernet and Smith, 1997; Häder et al., 1995, 1988; Häder and Liu, 1990; Häder and Griebenow, 1989; Häder, 1993; Nultsch and Agel, 1986; Smith, 1989; Voitek, 1990).

To assess the possible photobiological impact of solar UV-B and UV-A radiation on phytoplankton in the highly transparent waters of the subtropical Atlantic, bio-optical measurements were performed during the AZORES II cruise of the research vessel "Hesperides" in April 1999 with the following aims:

- determination of the optical properties of the waters and of the influence of attenuating substances (gelbstoff and seston) on the solar spectrum at different depths of the column
- characterization of the penetration of spectral solar irradiance into the water column as well as of broad-band (UVR and PAR) and of photobiologically effective solar irradiance as a function of the optical water type and of depth
- estimation of the exposure of marine micro organisms to solar UVR, PAR and to photobiologically effective solar radiation at the layer between the water surface and between the depth of maximum chlorophyll-*a* concentration.

2. Materials and methods

2.1. Stations

The investigations were performed in an area of the sub-tropical Atlantic Ocean between 21°W and

30°W, and 28°N and 36°N during the AZORES II cruise of the Spanish research vessel "Hesperides" in April 1999 (cf. Fig. 1).

2.2. Optical measurements

Using a temperature-stabilized double monochromator spectroradiometer (type 754, Optronic Lab., Orlando, FL, USA) the scalar solar irradiance was measured between 290 and 750 nm with a spectral resolution of 1 nm at different stations and at depths of the column between 1.0 and 10 m. To determine the scalar solar irradiance in the water column, a highly sensitive 4π sensor was connected to the entrance slit of the spectroradiometer by a 20-m quartz fiber cable (Piazena and Häder, 1997).

The deviation of the spherical response of the 4π sensor from the ideal distribution was between -13% and $+6\%$. The calibration of the instrument was performed by using an Ulbricht integrating sphere with an inner diameter of 55 cm, internally coated with Ba_2SO_4 and a 200 W tungsten standard lamp (Optronic Laboratories, Orlando, FL, USA). To exclude temperature-dependent errors and wavelength shifts, the monochromator was stabilized by a thermostat, which warrants a nearly constant temperature of the monochromator of (25 ± 2)°C for external temperatures between 0°C and 40°C. Before starting each series of measurements, the wavelength shift was determined and corrected by using the 296.73-nm line of a mercury lamp. A field intercomparison of spectroradiometers at Garmisch-Partenkirchen/Germany in August 1997 showed a long-term wavelength shift of <0.2 nm and an agreement with the data of the reference instrument between -5% and $+8\%$ for erythemal UV and within $\pm5\%$ for UV-A (Seckmeyer et al., 1998). To exclude errors due to significant changes of solar elevation above horizon and of the meteorological conditions, the series of spectral measurements at different depths of the water column were performed between 2 h before and after local noon within 30 min and under nearly constant atmospheric transparency. In the case of significant changes of the meteorological conditions during the spectral radiometric measurements, the data were excluded from the analysis. In addition, the measurements were carried out exclusively from the vessel side directed to the sun using an extender of 3 m length to avoid errors caused by reflections or shading effects. Thus, the measurement errors of scalar spectral irradiance are $<\pm15\%$, causing uncertainties of the calculated attenuation coefficients of about $\pm21\%$. In addition to each series of spectroradiometric measurement, the visual depth was determined by using a Secchi disk. To verify the data of solar irradiance calculated for deeper parts of the photic zone derived from the spectroradiometric measurements in the near-surface layer, the downward irradiance was measured directly as a function of depth at four different bands in the UV range as well as in the PAR by using a submersible probe (type PUV-500, Biospherical Instruments Inc., San Diego, CA, USA). The measurements were performed synchronously and under conditions which were comparably to the spectroradiometric measurements.

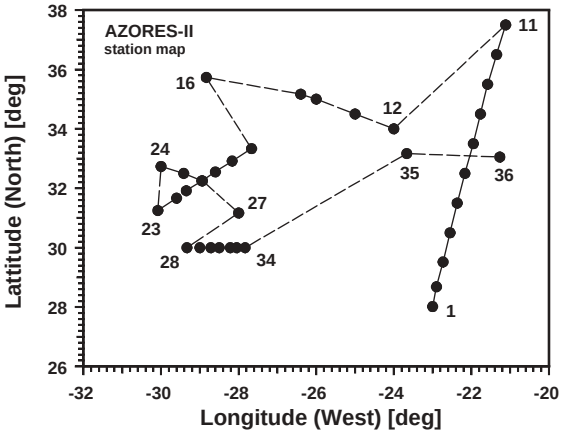

Fig. 1. Station map of the research vessel "Hesperides" during the AZORES-II cruise in April 1999.

2.3. Attenuating substances and phytoplankton

To determine the contents of gelbstoff and seston, 3-l water samples were taken at each station at depths of 5 m and at the depths of the maximum concentration of chlorophyll *a*, which were derived from direct measurements of the

vertical distribution of the organisms in the column using a probe for the excitation of characteristic chlorophyll *a* fluorescence (excitation wavelength: 425 nm, emission wavelength: 685 nm, range: 0–30 mg m^{-3}). The fluorometer was integrated in the CTD probe (type MARK-III, General Oceanics, USA) of the "Hesperides", which also contained bottles for water sampling. Both the data of the depths of maximal chlorophyll *a* concentration as well as the water samples of different depths were provided by the technical crew of the research vessel. The water samples were filtered by using GF/F and GTTP filters (0.6 and 0.2 μm, Whatman International Ltd., Maidstone, England). The seston concentration was derived from the difference of the filter dry weights before and after filtrating. The contents of yellow substances was characterized by the reduced spectral absorption coefficients which were defined by the difference between the spectral absorption coefficients of the filtered water samples and of distilled water. The measurements were performed using a quartz cuvette with 10 cm length in a scanning spectrophotometer in the wavelength range between 200 and 700 nm (UVICON 800, Kontron Analytik GmbH, Eching/Munich, Germany).

2.4. Calculations

Based on data of the spectral scalar irradiance $E_{0\lambda}(z_i)$ at different depths z_i were calculated:

- the *spectral attenuation coefficients* for scalar irradiance $K_{0\lambda}$ using

$$K_{0\lambda} = -\Delta z^{-1} \ln[E_{0\lambda}(z_i)/E_{0\lambda}(z_{i-1})], \quad (1)$$

  where $\Delta z = z_i - z_{i-1}$ defines the vertical distance between the two depths between $i = 1$, 3, 5, 7 and 10 m,
- the *spectral depths of penetration* to 1% of the sub-surface irradiance

$$d_{1,\lambda} = -(K_{0\lambda})^{-1} \ln 0.01 \quad (2)$$

  under the assumption of vertical homogeneously distributed attenuating substances and
- the *scalar broad-band irradiance* ($E_{0,b}$) for the wavelength ranges UV-B ($E_{\mathrm{UV-B}}$), UV-A ($E_{\mathrm{UV\text{-}A}}$) and PAR (E_{PAR}) as a function of depth by integration in the wavelength intervals 290–315 nm (UV-B), 315–400 nm (UV-A) and 400–700 nm (PAR) according to

$$E_{0,\mathrm{b}}(z_i) = \sum_{\lambda} [E_{0\lambda}(z_{i-1})(\mathrm{e}^{(-K_{0\lambda}\Delta z)})]\Delta\lambda, \quad (3)$$

  where $\Delta\lambda$ defines the step width in the spectral measurement
- the *effective scalar irradiance* for DNA damage (E_{DNA}, Setlow, 1974), for the stimulation of photosynthesis (E_{PS}, DIN 5031/10, 1996) and for the inhibition of photosynthesis (E_{PSI}, Jones and Kok, 1966) at the depth z_i by spectral weighting the data of spectral scalar irradiance $E_{0\lambda}$ with the generalized action spectrum $s_{x\lambda}$ of each effect (x, cf. Fig. 2) and integration between its spectral limits according to

$$E_{0,x}(z_i) = \sum_{\lambda} [E_{0\lambda}(z_i) s_{x\lambda}]\Delta\lambda. \quad (4)$$

  (In contrast to the definition of E_{PS} which covers the total spectral range of photosynthetically effective radiation (cf. Fig. 2), E_{PSS} characterizes the effective irradiance for the

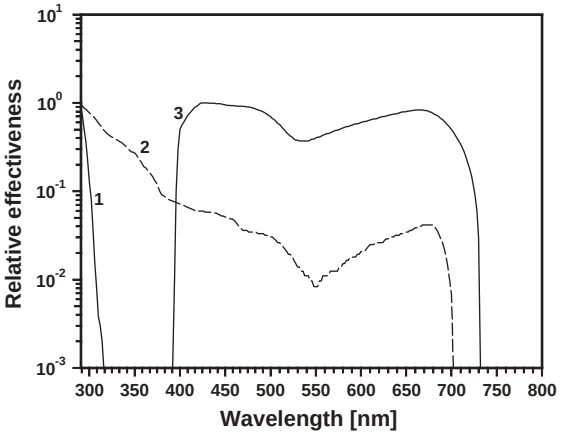

Fig. 2. The relative effectiveness of DNA damage (Setlow, 1974) (1), of the photoinhibition of photosynthesis (DIN 5031/10, 1996) (2), and of the stimulation of photosynthesis (Jones and Kok, 1966) (3) as a function of wavelength. (Note that the action spectra 2 and 3 are generalized examples. Their slopes are quite different depending on the kind of organisms and conditions.)

stimulation of photosynthesis in the short-wavelength range below 540 nm.)

Because spectral changes of the solar spectrum with depth exclude the definition of a "attenuation coefficient of broad-band irradiance" (Booth and Morrow, 1997) according to the Eqs. (2) and (3), the depths of penetration to 1% of the sub-surface irradiance of solar UVR and PAR as well as of effective solar radiation were derived directly from the slopes of their vertical profiles in the water column calculated for different depths of the photic zone according to the Eqs. (3) and (4).

The data of spectral irradiance which were scanned with spectral steps of 2 nm were interpolated to spectral steps of 1 nm to avoid errors in the calculation of data of UV-B irradiance as well as effective irradiance of DNA damage.

3. Results

3.1. Optical properties and penetration of solar irradiance into the water column

The characterization of the optical properties of the waters at each station is based on the analysis of:

- the spectra of the scalar irradiance measured at different depths in the near-surface layer as well as extrapolated for depths to 200 m according to Eq. (3),
- the spectral attenuation coefficients calculated according to Eq. (1), which were compared with the slopes of spectral attenuation coefficients defined for different water types in the Jerlov system of optical classification,
- the depth of penetration to 1% of the spectrally sub-surface values of irradiance, and
- vertical profiles of the broad-band irradiance in the ranges of UV-B, UV-A and PAR and of the effective irradiance for DNA damage, photosynthesis and for the inhibition of photosynthesis, which were used to estimate the related depths of penetration to 1% of the sub-surface broad-band irradiance ("1% depths" for UVR and for PAR).

For instance, a complete set of these data for station 26 is shown in Fig. 3.

3.2. Spectral characteristics and optical classification

The spectral attenuation coefficients derived for the investigated stations slope within the limits of the slopes of the spectral attenuation coefficients for the oceanic water types OI–OIII in the Jerlov system of classification (Fig. 4). However, especially for the stations 1–11 deviations from the concentrations and from the composition of attenuating substances and microorganisms assumed in the Jerlov system caused a crossover between the determined spectra of the attenuation coefficient as well as between the spectral slopes predicted for different water types. Thus, whereas the spectral attenuation coefficients derived for these stations are similar to the slopes of the water types OIB and OII in the UV and in the short-wavelength range of PAR ($\approx$290–450 nm), they slope within the limits of the types OII and OIII in the long-wavelength range of PAR ($\approx$450–700 nm).

In contrast, the slopes of the spectral attenuation coefficients observed at the stations 13–33 indicate waters of higher transparency, which varies within the limits of the types OIB–OI in the whole range of the spectrum.

The calculation of the spectral depths of penetration to 1% of the sub-surface irradiance according to Eq. (2) results in spectral slopes shown in Fig. 5 for the stations investigated and summarized in Table 1 for the wavelengths 310 nm, 400 nm and for the maximum of transmission.

3.3. Attenuating substances

As shown in Figs. 6–8, the contribution of particulate and dissolved substances to the attenuation of solar radiation in the column is small. The concentration of seston shows only insignificant changes in the column at each station between 5 m depth and the maximum depth of chlorophyll *a* concentration. In addition, the differences between different stations are insignificant. Thus, the waters in all areas investigated are interspersed by seston in their photic layers to a

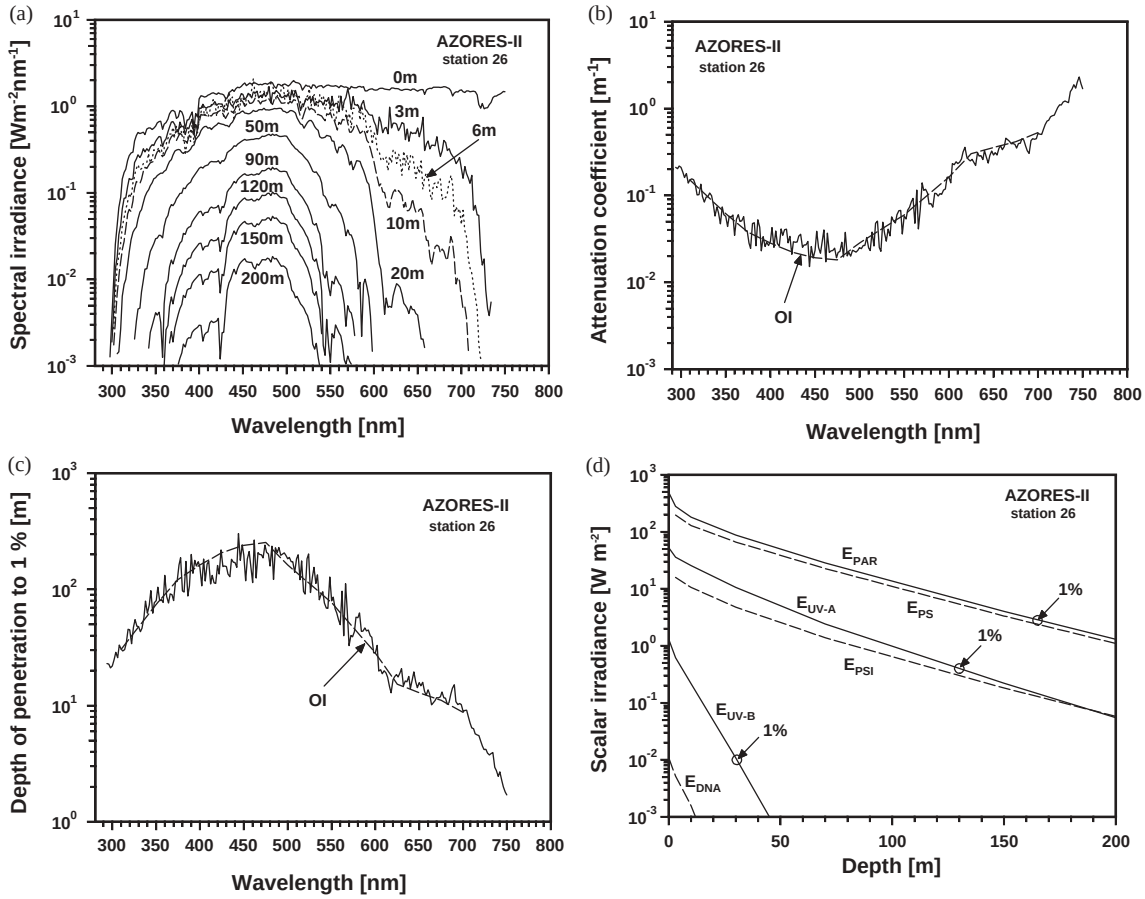

Fig. 3. Optical characterization of the water at station 26: (a) spectral scalar irradiance above the sea surface (0 m) and at different depths (measured data: 3 and 6 m, calculated data: 10–200 m, (b) spectral attenuation coefficients calculated between depths of 1, 3 and 6 m in comparison with the spectral attenuation coefficient for oceanic water of type I (Jerlov system), (c) depth of penetration of subsurface solar irradiance to 1% as a function of wavelength, and (d) scalar solar irradiance in the ranges UV-B ($E_{\mathrm{UV\text{-}B}}$), UV-A ($E_{\mathrm{UV\text{-}A}}$), and PAR (E_{PAR}) and effective irradiance for DNA damage (E_{DNA}), for the stimulation of photosynthesis (E_{PS}), and for the inhibition of photosynthesis (E_{PSI}) in dependence of depth.

similar extent showing a mean concentration of about $(8.6 \pm 0.6)\,\mathrm{mg\,l^{-1}}$ (Fig. 6).

To analyze the effect of micro-substances and microorganisms with diameters smaller than 0.6 μm on the attenuation of solar radiation in the water column, the reduced spectral absorption coefficients were determined at five different stations for both water samples. However, whereas differences were found between different depths, the comparison of the reduced spectral absorption coefficients for water samples filtered by GFF filters and by GTTP filters shows only insignificant differences (Fig. 7). Thus, the determination of the effect of dissolved substances at each station was based on the analysis of reduced spectral absorption coefficients derived from water samples filtered by GFF filters only. The reduced absorption coefficients depicted in Fig. 8 at wavelengths of 275, 300 and 325 nm show

- a decreasing trend with the number of station
- higher values at the depths of maximal chlorophyll *a* concentrations in comparison with the data given in the near-surface layer (cf. Table 2)
- small values in the UV-B range for the stations 1–15 (water types OII–OIB), but small or

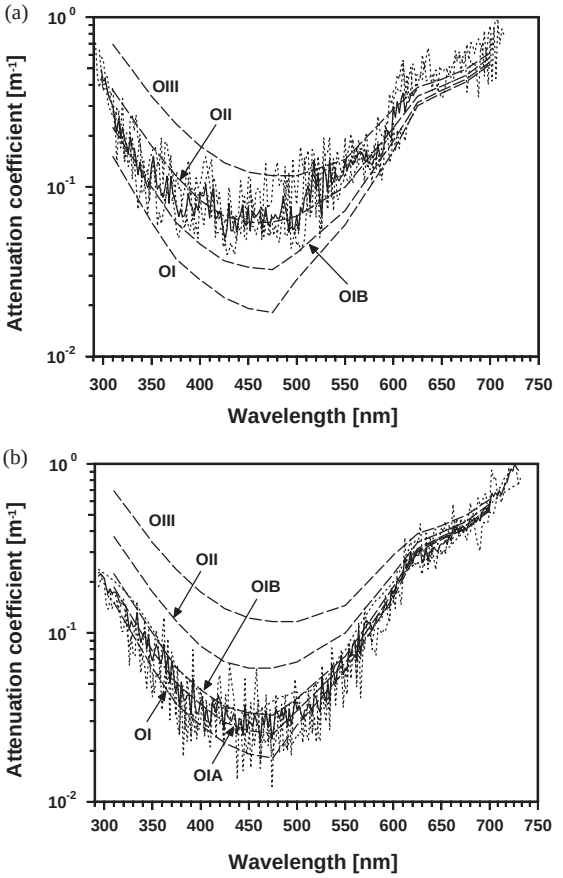

Fig. 4. Spectral attenuation coefficients for scalar irradiance as a function of wavelength in comparison to the coefficients characterizing oceanic water of the type OI, OIA, OIB, OII and OIII (Jerlov system); stations 1–11 (a) and stations 13–33 (b) (.....): single spectra (—): averaged spectra.

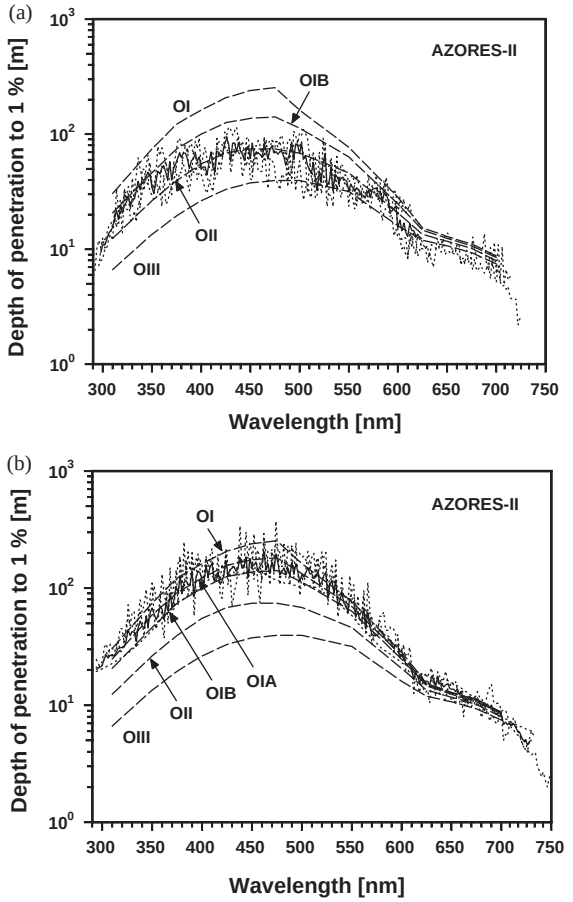

Fig. 5. Spectral depths of penetration to 1% of the sub-surface irradiance as a function of wavelength in comparison with the related depths characterizing oceanic water of the type OI, OIA, OIB, OII and OIII (Jerlov system); stations 1–11 (a) and stations 13–33 (b); (.....): single spectra (—): averaged spectra.

negligible values for the stations 18–33 (water types OIB–OI, cf. Table 2).

3.4. Depths of penetration to 1% of the sub-surface irradiance for PAR and UVR

As shown in Figs. 6 and 8 the absolute contents and vertical changes of the concentration of attenuating substances are small or negligible in the waters investigated. In addition, Fig. 9a compares solar irradiance data measured at station 26 at the wavelengths of 305, 320, 340, and 380 nm and in the range of PAR by using a submersible probe (type PUV-500) with the slopes calculated for solar UVR and PAR. Using a semi-logarithmic scale, both the irradiance data detected spectrally by the probe as well as calculated in the UV range decrease linearly with depth in the whole layer investigated. However, according to Eq. (1) these slopes result in constant values of the spectral attenuation coefficient with depth in the whole column investigated. Furthermore, both the calculated and directly measured data of solar PAR indicate similar slopes with depth deviating from each other by $<10\%$ (Fig. 9b).

Thus, both results shown in Figs. 6 and 8 as well as in Fig. 9 support the assumption of a sufficient approximation to the condition of an optically

Table 1
The depth of penetration to 1% of the sub-surface spectral irradiance at the wavelengths 310 nm, 400 nm and at the spectral maximum of transmission (450–500 nm) for the stations 1–11 and 13–33 and for the oceanic water types OI–OIII in the Jerlov system of classification

Wavelength (nm)	Spectral depth of penetration to 1% of the sub-surface irradiance (m)						
	Stations		Jerlov water types (oceanic)				
	1–11	13–33	OI	OIA	OIB	OII	OIII
310	12–18	20–30	30.5	24.7	20.6	12.4	6.6
400	45–55	100–156	162.2	122.1	100.0	55.2	26.4
450–500	50–82	105–191	253.5	181.9	141.1	74.4	39.5

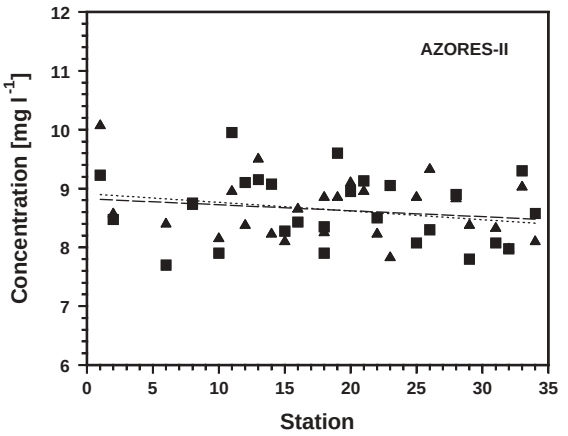

Fig. 6. The concentration of seston at a depth of 5 m (■, ----) and at the depth of the maximum of chlorophyll *a* concentration (▲, ...) in dependence of the station of sampling.

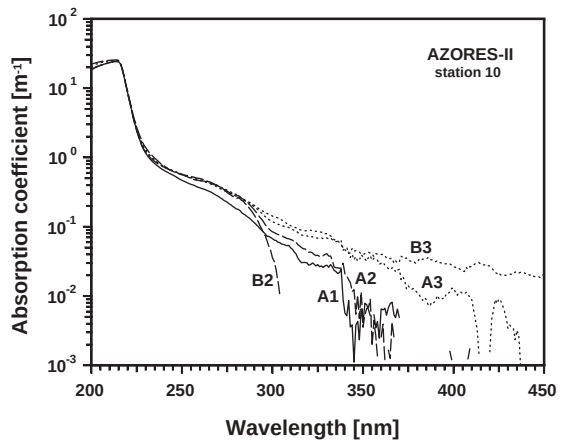

Fig. 7. Reduced spectral absorption coefficients of water samples of station 10 filtered by using GF/F filters (A) and GTTP filters (B) for sampling depths at 5 m (1), 30 m (2) and 65 m (maximum of chlorophyll *a* concentration, 3).

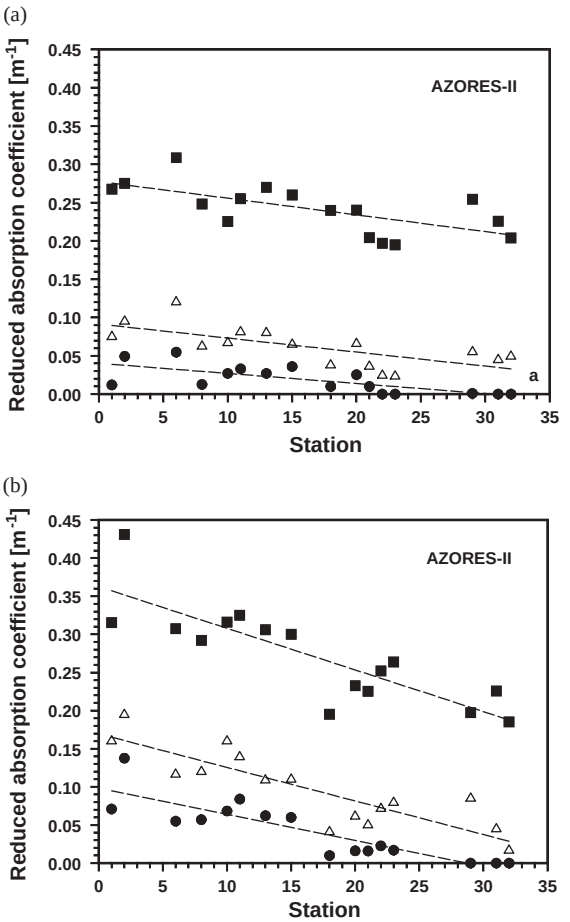

Fig. 8. Reduced spectral absorption coefficients of GF/F filtered water samples at wavelengths of 275 nm (■), 300 nm (△) and 325 nm (●) for sampling depths at 5 m (a) and at the maximum of chlorophyll *a* concentration (b) in dependence of the number of station.

Table 2
Range of the reduced spectral absorption coefficient of GF/F filtered water samples at wavelengths of 275, 300 and 325 nm for sampling depths at 5 m and for the depth of maximal chlorophyll *a* concentration summarized for the stations 1–15 and 18–33

Wavelength (nm)	Reduced absorption coefficient (m^{-1})			
	Near-surface layer (depth of 5 m)		Depth of chlorophyll maximum (depths between 60 and 120 m)	
	Stations 1–15	Stations 18–33	Stations 1–15	Stations 18–33
275	0.22–0.31	0.19–0.26	0.29–0.43	0.20–0.27
300	0.06–0.12	0.03–0.06	0.12–0.20	0.02–0.09
325	0.02–0.06	0.00–0.03	0.06–0.14	0.00–0.02

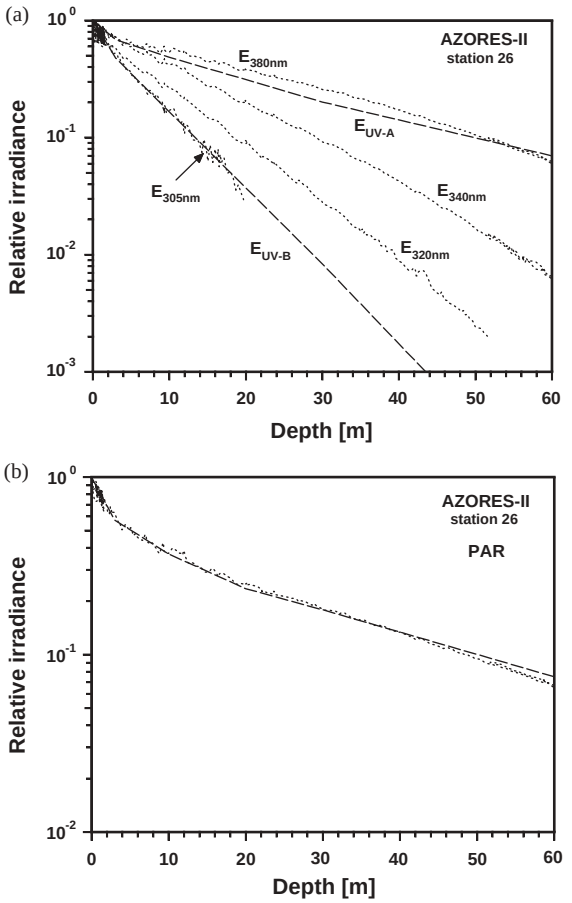

Fig. 9. The relative solar irradiance at different wavelengths in the UV range (a) and in the photosynthetic active range PAR (b) as a function of depth; dotted lines: directly measured data at 305, 320, 340, 380 nm and of PAR by using a submersible probe (type PUV-500); dashed lines: calculated data in the ranges UV-B, UV-A and PAR according to Eq. (3) by using the spectral attenuation coefficient (cf. Fig. 3c) derived from synchronous measurements with the OL 754 spectroradiometer in the near-surface layer.

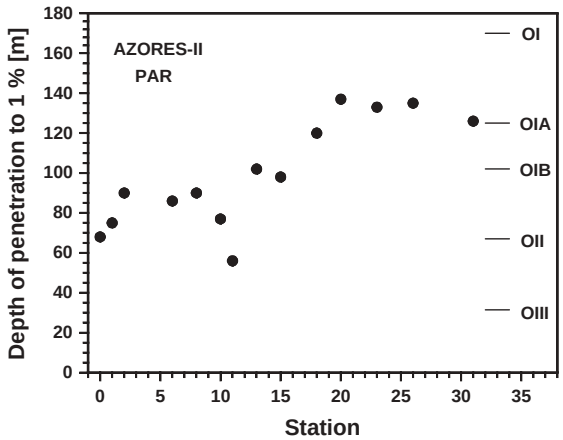

Fig. 10. Depths of penetration to 1% of the sub-surface irradiance for PAR for the stations investigated and for the water types OI–OIII in the Jerlov system of classification.

homogeneous water column that is necessary to extrapolate the irradiance data of solar UVR and PAR from measurements in the near-surface layer to deeper layers of the photic zone according to Eq. (3).

For both the 1% depths of PAR and UVR were found increasing values during the cruise. The 1% depths of PAR vary between 55 and 100 m for stations 1–15, whereas for stations 18–31 values between 100 and 140 m were derived from the vertical profiles calculated according to Eq. (3) (cf. Fig. 10). Comparing these data with the 1% depths of PAR for the oceanic water types OI–OIII of the Jerlov system a classification of the waters investigated is suggested into the types OII–OIB for stations 1–15 and into the types OIB–OIA for stations 18–31.

The penetration of UVR into the water column was characterized as ratio between the 1% depths

of UVR and PAR. Fig. 11 shows increasing values during the cruise, which vary between 0.17 and 0.32 for the ratio UV-B/PAR and between 0.50 and 0.94 for the ratio UV-A/PAR. Thus, solar UV-B penetrates the photic zone which is limited by the 1% depth of PAR up to about 25% whereas for UV-A values up to about 75–93% were found.

3.5. Visual depth

The data of the visual (Secchi) depth vary between about 14 and 23 m for stations 0–11 and show increasing values for stations 13–28 which are between about 27 and 44 m (cf. Fig. 12).

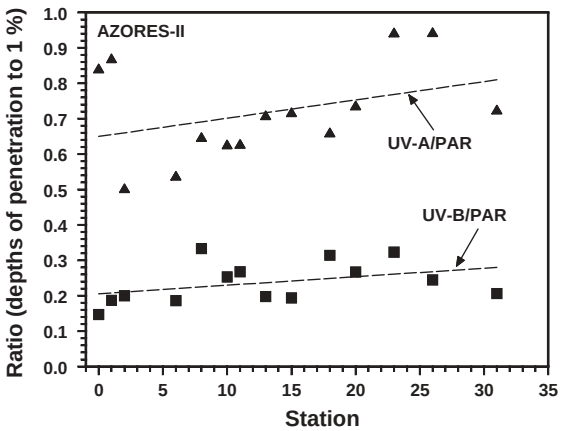

Fig. 11. The depths of penetration to 1% of the sub-surface irradiance in the UV-B and UV-A range in comparison with the 1% depth of PAR in dependence of the number of station.

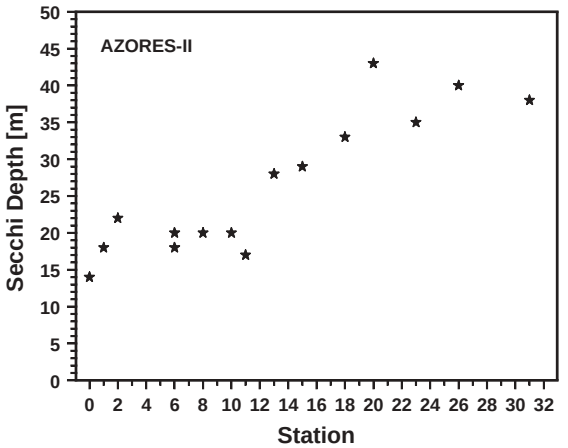

Fig. 12. The visual (Secchi) depth in dependence of the number of station.

4. Discussion

4.1. Optical properties and optical characterization

The investigated waters are characterized by small or negligible concentrations of gelbstoff and by small but detectable contents of particulate substances. However, differences in their composition and the ingredients of attenuating matter assumed in the definition of different water types in the Jerlov system result in a crossover of the observed spectra of the attenuation coefficient with the defined spectral slopes of different optical types (cf. Fig. 4). Consequently, the classification of the investigated waters into water types of the Jerlov system has to be specified for the spectral range. For instance, the slopes of the spectral attenuation coefficients derived for all investigated stations indicate a decreased transparency in the range of about 400–550 nm (short-wavelength PAR) as compared with the transparency in the UV range, which can be quantified into types of the Jerlov system and which extend to the order of about one water type. Moreover, Fig. 4a shows spectra of the attenuation coefficient that slope similarly with type OIB in the UV range but significantly exceed the limit of type OII in the long-wavelength range of PAR.

On the other hand, the assessment of optical properties in the UV range by water types in the Jerlov system may result in a significant misjudgment if the data are derived from transmission measurements in the PAR range. For example, Fig. 10 suggests optical properties in the PAR range for station 26 that are equivalent to type OIA, whereas the spectra depicted in Fig. 3b slope similarly to type OI in the UV range.

4.2. Visual depth and the 1% depth of PAR

As shown in Fig. 13, the visual (Secchi) depth (d_{DS}) and the depth of transmission to 1% of the sub-surface irradiance in the PAR range ($d_{1,PAR}$) are highly correlated ($r = 0.92$). Thus, the 1%

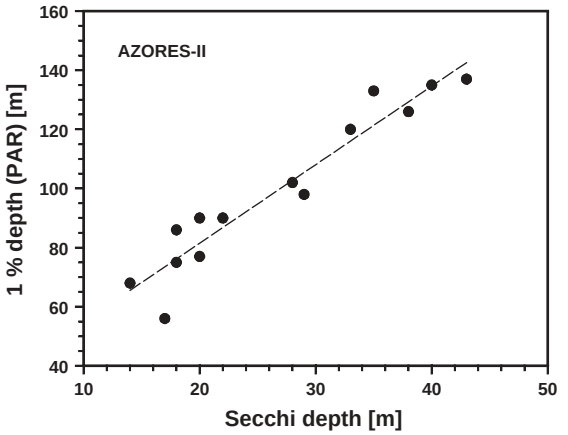

Fig. 13. The depth of transmission to 1% of the sub-surface irradiance in the PAR range as a function of the visual (Secchi) depth.

depth of PAR ($d_{1,\mathrm{PAR}}$= [m]) may be estimated as a first approximation by simple measurements of the Secchi depth (d_{DS}= [m]) according to

$$d_{1,\mathrm{PAR}} \approx 2.76 d_{\mathrm{DS}} + 28.43. \quad (5)$$

However, the use of Eq. (5) is restricted to oceanic waters showing similar optical properties and to Secchi depths between about 10 and 45 m. As noted in the oceanographic literature (Hoerslev, 1986; Kirk, 1994) and as reflected in Fig. 14a, the ratio $A = d_{1,\mathrm{PAR}}/d_{\mathrm{DS}}$ depends on the optical water type, which was found to change during the cruise from the Jerlov types OII–OIB for the stations 1–11 to the types OIB–OIA for the stations 13–31 (cf. Fig. 10). Thus, the data of the ratio A show a decreasing trend with the station number between about 4.8 and 3.2, whereas the equivalent ratio $B = -\ln 0.01/A$ increases between about 0.96 and 1.44 (Fig. 14b). The values are on the same order as data published to estimate the average vertical attenuation coefficient of downward irradiance of solar PAR according to

$$K_{d,\mathrm{PAR}} = B/d_{\mathrm{DS}}. \quad (6)$$

The data of the parameter B listed by Hoerslev (1986) for different oceanic waters range between 0.3 and 1.7.

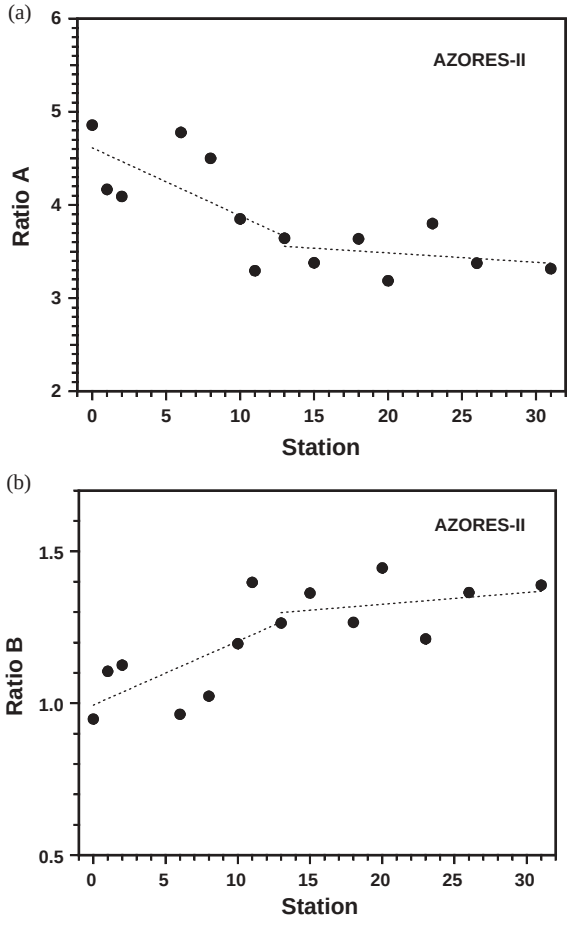

Fig. 14. The ratios A (a) and B (b) in dependence of the number of station.

4.3. Photobiological impact

The biological effects of UVR and PAR on microorganisms populating the waters strongly depend on their spectra, which are modified with depth by absorption and scattering processes at water molecules and contained substances. Thus, both UVR and PAR not only show a decrease of irradiance with depth but also a change of their spectral composition. Consequently, these spectral changes limit the characterization of biological effectiveness of solar radiation by irradiance data of UVR and PAR at different depths.

To estimate the effectiveness of both solar UVR and PAR on phytoplankton and marine micro-

organisms as well as to analyze the differences between unweighted irradiance data and data of effective irradiance weighted by the action spectra of different biological effects (cf. Fig. 2), the following entities were compared for different stations independence of depth.

- the 1% depth of PAR with the depth of maximum concentration of chlorophyll *a*;
- the effective irradiance of photosynthesis (E_{PS}) with the irradiance in the photosynthetic active range of the spectrum (E_{PAR});
- the effective irradiance of the inhibition of photosynthesis (E_{PSI}) with the effective irradiance of photosynthesis (E_{PS}); and
- the penetration of effective irradiance of DNA damage with the penetration of solar (unweighted) irradiance in the UVB range.

Fig. 15 shows that the majority of the organisms that constitute the phytoplankton community in the column are found between the surface and the 1% depth of PAR. The organisms are distributed in the photic zone showing maxima of their concentrations at layers that are transmitted by photosynthetic active irradiance (PAR) of about 10–80 $W m^{-2}$. However, due to the spectrally dependent attenuation of solar radiation with depth, the PAR, which covers the wavelength

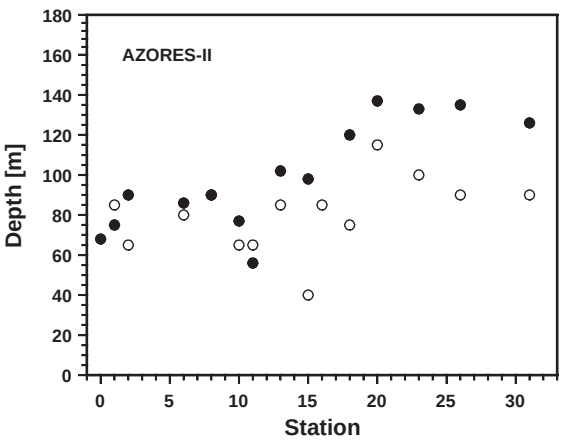

Fig. 15. The depth of transmission to 1% of the sub-surface irradiance in the PAR range (full circles) and the depth of the maximal chlorophyll *a* concentration (○) in dependence of the station number.

range between 400 and 700 nm is reduced at the depths of maximal chlorophyll *a* concentrations into the sub-range between about 430 and 510 nm (cf. Fig. 3a). Thus, the photon irradiance of solar radiation calculated at the central wavelength (470 nm) of this spectral sub-range (Tevini and Häder, 1985) varies at the depths of the maximal chlorophyll *a* concentration for all stations between about 3 and 20 $\mu mol\, m^{-2}\, s^{-1}$.

In contrast to the definition of PAR, which encloses all contributing wavelengths in the range between 400 and 700 nm without spectral weighting, the photosynthetically effective radiation is weighted by the action spectrum of photosynthesis, which shows two maxima (half-band widths between 400 and 515 nm as well as between 576 and 700 nm) that are mainly caused by light absorption by chlorophyll *a*, chlorophyll *b* and carotenoids.

Thus, the spectral slopes of (unweighted) solar irradiance (cf. Fig. 3a) typically differ from the spectra of photosynthetically effective irradiance, which for comparison are shown in Fig. 14a for station 26. With the exception of the range between 430 and 440 nm, the weighted spectral data are generally reduced in comparison with the unweighted data showing a minimum of photosynthetic effectiveness at wavelengths between about 530 and 560 nm.

However, the differences between the data of (unweighted) solar irradiance in the photosynthetic active range (E_{PAR}) and between the photosynthetic effective irradiance (E_{PS}) depend on depth. As shown in Fig. 17a for different stations and for the Jerlov water types OI–OIII, the ratio E_{PS}/E_{PAR} decreases with depth from about 0.7 in the near-surface layer to about 0.9 at deeper layers of the photic zone. The ratio E_{PS}/E_{PAR} is also determined by the water type (Fig. 17a).

Moreover, Fig. 16a suggests an increasing influence of short-wavelength radiation (wavelengths below 540 nm, E_{PSS}) with depth upon the total photosynthetically effective irradiance (E_{PS}) in comparison with the contribution in the long-wavelength range (wavelengths above 540 nm), which is caused by the spectrally dependent attenuation of optical radiation in the

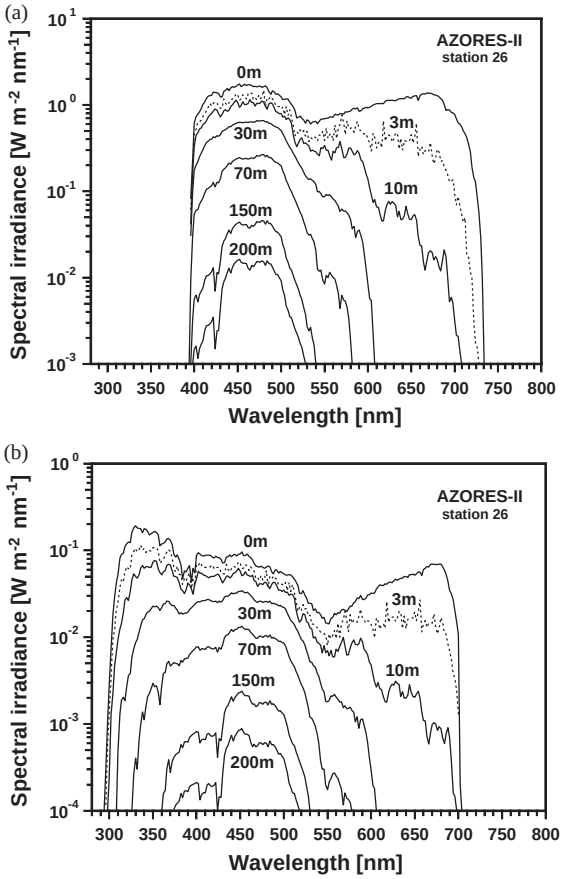

Fig. 16. The effective scalar irradiance of the stimulation of photosynthesis (a) and of the photoinhibition of photosynthesis (b) at station 26 as a function of wavelength above the sea surface (0 m) and at different depths between 3 and 200 m.

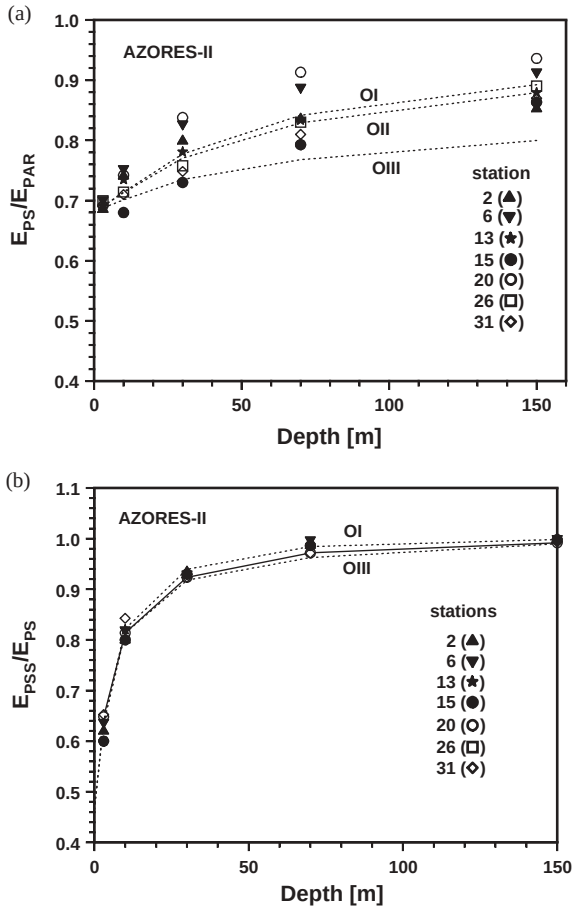

Fig. 17. The ratio E_{PS}/E_{PAR} (a) and the ratio E_{PSS}/E_{PS} (b) as a function of depth at the different stations and for the oceanic water types OI and OIII.

water column. The ratio E_{PSS}/E_{PS}, which shows negligible changes with the optical type of oceanic waters, strongly depends on depth and varies between about 0.6 in the near-surface layer and 1.0 at deeper layers of the column (Fig. 17b). Thus, whereas both short-wavelength as well as long-wavelength photosynthetically effective radiation is available for the organisms which populate the near-surface part of the photic zone, the organisms at deeper layers have to perform photosynthesis only with short-wavelength radiation. Consequently, these changes in the spectral quality of photosynthetically active radiation with depth may contribute to a selection of the kind of species in the column.

The action spectra depicted in Fig. 2 indicate that optical radiation in both the ultraviolet and in the photosynthetic active ranges of the spectrum may inhibit the photosynthetic production by the organisms. However, the spectral slopes of effective solar irradiance for the photoinhibition of photosynthesis shown in Fig. 16b for station 26 are characterized by significant differences from the spectra of the photosynthetically effective irradiance (Fig. 16a) which depend on depth due to the wavelength dependence of attenuation. Mainly the comparatively strong attenuation of

UVR in the water column causes a relative decrease of the effective irradiance for photoinhibition of photosynthesis (E_{PSI}) with depth, which exceeds the relative decrease of the photosynthetically effective irradiance (E_{PS}) with depth. The ratio E_{PSI}/E_{PS}, which was calculated for different stations as well as for the Jerlov water types OI–OIII, decreases with depth between the surface and the 1% depth of PAR by about 30% for waters of the type OI and by about 40% for waters of the types OII and OIII (Fig. 18). Thus, the limiting influence of photoinhibition upon the photosynthetic production of phytoplankton decreases significantly with depth.

To compare the penetration of effective solar irradiance of DNA damage into the water column with the penetration of (unweighted) solar irradiance in the UV-B range the 1% depths of both irradiance data were calculated. Fig. 19 shows the 1% depths of effective irradiance of DNA damage for the Jerlov water types OI–OIII, which are systematically smaller than the 1% depths of solar UV-B irradiance. Thus, the effectiveness of solar radiation to damage the DNA of organisms in the water column is overestimated if data of the penetration of (unweighted) solar UV-B irradiance are used. However, the differences vary only within 20% and are usually smaller than the error of the measurement. In agreement with

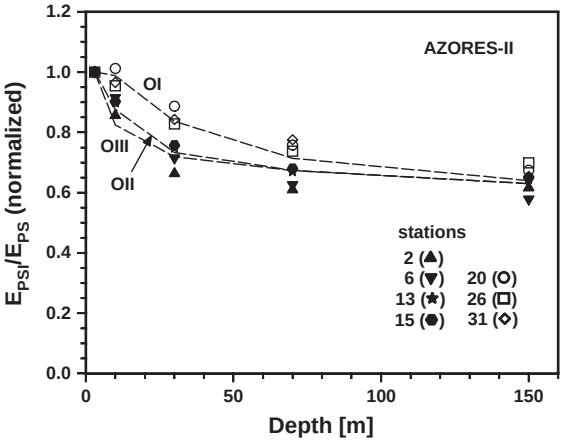

Fig. 18. The ratio E_{PSI}/E_{PS} as a function of depth at the different stations and for the oceanic water types OI, OII and OIII (normalized to the ratio at the sub-surface).

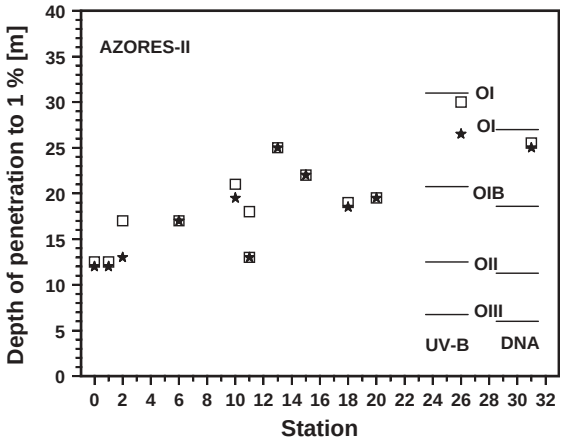

Fig. 19. The depth of penetration to 1% of the sub-surface solar irradiance in the UV-B range (squares) and of the effective solar irradiance of DNA damage (stars) for the stations investigated and for the oceanic water types OI–OIII in the Jerlov system of classification.

these results, the 1% depths of solar UV-B irradiance and of the effective irradiance of DNA damage determined for each station investigated show only differences that are insignificant or amount to $<20\%$ (Fig. 19). Consequently, data of the penetration of (unweighted) solar irradiance in the UV-B range are suitable to estimate the effectiveness of solar radiation to damage the DNA of organisms in the photic zone of oceanic waters.

As shown in Fig. 11 solar UV-B radiation penetrates the waters investigated in dependence of the water type to about 17–32% of the photic zone, whereas solar UV-A radiation penetrates to about 50–94%. Thus, solar UVR may significantly affect and damage the majority of the organisms that populate the photic zone. However, in most cases the maxima of chlorophyll *a* concentration were found at depths below 50 m in the column. Thus, whereas the organisms in the near-surface layer are exposed to both the UV-B and the UV-A component of solar irradiance, the photobiological effectiveness of solar UVR upon the majority of the organisms, which are concentrated at deeper layers of the photic zone is restricted to the impact of the UV-A component. Thus, the impact of solar radiation to stimulate damaging effects mainly

caused by UV-B radiation such as DNA damage and inhibition of motility is limited to the organisms populating the near-surface layer. Consequently, the differences of penetration of solar UV-B and UV-A into the water column may cause both changes of the kind of species with depth as well as responses of the organisms such as the induction of synthesis of UV protective pigments (e.g., mycosporins). Fig. 20 shows an additional peak in the UV range of the absorption spectra of the chlorophyll samples of station 10, which was only observed for the organisms sampled in the near-surface layer, which indicates either the formation of UV protective pigments or a change in the species composition in the water column.

However, the role of solar UVR as a selection factor for the species in the water column is not only based on effectiveness of the UV-B component but also on the photobiological impact of UV-A that may contribute significantly to chlorophyll bleaching as well as to the decrease of the photosynthetic activity. As shown in Fig. 16b, the effectiveness of solar UV-A irradiance upon the photoinhibition of photosynthesis significantly exceeds the effectiveness of the UV-B component even in the near-surface layer of the column. However, whereas the results derived above are restricted to possible biological effects of solar UVR and PAR on phytoplankton at different depths the assessment of the real effects upon single organisms and upon the marine ecosystem requires further research (Booth et al., 1997; Smith, 1989), which involves the influence of additional factors and of their combinations such as exposure times at different depths and migration of the organisms in the water column, adaptation processes and repair effects as well as interactions of the species and nutrients.

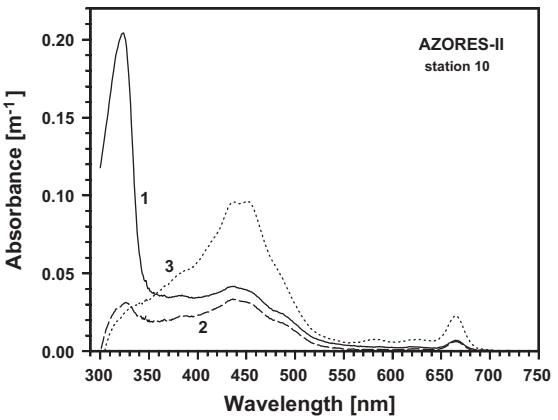

Fig. 20. The absorbance of water samples as a function of wavelength sampled at station 10 at depths of 5 m (1), 50 m (2) and at the depth of maximal chlorophyll *a* concentration (3).

Acknowledgements

The investigation was supported by the Commission for the European Community (MAS3CT960060). We thank Dr. Emilio Fernandez (chief scientist and leader of the AZORES-II expedition, Universidad de Vigo, Spain, Don José María Turnay Abad (captain of the research vessel "Hesperides") and his crew for generous support of the investigation.

References

Booth, C.R., Morrow, J.H., 1997. The penetration of UV into natural waters. Photochemistry and Photobiology 65, 254–257.

Booth, C.R., Morrow, J.H., Coohill, T.P., Cullen, J.J., Frederick, J.E., Häder, D.-P., Holm-Hansen, O., Jeffrey, W.H., Mitchell, D.L., Neale, P.J., Sobolev, I., van der Leun, J., Worrest, R.C., 1997. Invited review: impacts of solar UVR on aquatic microorganisms. Photochemistry and Photobiology 65, 252–269.

DIN 5031, Teil 10, 1996. Strahlungsphysik im optischen Bereich (Ultraviolett, Licht, Infrarot)—Größen, Formel- und Kurzzeichen für biologisch wirksame Strahlung. Beuth-Verlag, Berlin.

Häder, D.-P., 1993. Effects of enhanced solar ultraviolet radiation on aquatic ecosystems. In: Tevini, M. (Ed.), UV-B Radiation and Ozone Depletion. Lewis Publishers, Boca Raton, Ann Arbor, London, Tokyo, pp. 155–192.

Häder, D.-P., Liu, S.M., 1990. Motility and gravitactic orientation of the flagellate *Euglena gracilis*, impaired by artificial and solar UV-B radiation. Current Microbiology 21, 161–168.

Häder, D.-P., Reinecke, E., 1991. Phototactic and polarotactic responses of the photosynthetic flagellate *Euglena gracilis*. Acta Protozoology 30, 13–18.

Häder, D.-P., Rhiel, E., Wehrmeyer, W., 1988. Ecological consequences of photomovement and photobleaching in the

marine flagellate *Cryptomonas maculata*. FEMS Microbiology and Ecology 53, 9–18.

Häder, D.-P., Griebenow, K., 1989. Orientation of the green flagellate, *Euglena gracilis*, in a vertical column of water. FEMS Microbiology and Ecology 53, 159–167.

Häder, D.-P., Worrest, R.C., Kumar, H.D., 1994. Effects of increased solar ultraviolet radiation on aquatic ecosystems. UNEP Environmental Effects of Ozone Depletion, United Nations Environment Programme, Nairobi, Kenya, pp. 65–77.

Häder, D.-P., Worrest, R.C., Kumar, H.D., Smith, R.C., 1995. Effects of increased solar ultraviolet radiation on aquatic ecosystems. Ambio 24, 174–180.

Hoerslev, N.K., 1986. Optical properties of sea water. In: Sündermann, J. (Ed.), Landoldt-Bjornstein, Numerical data and functional relationships in science and technology, New Series V/3a, Springer, Heidelberg, Berlin, New York, pp. 383–462.

Jerlov, N.G., 1970. Light—General introduction. In: Kinne, O. (Ed.), Marine Ecology. Vol. 1, pp. 95–102.

Jerlov, N.G., 1976. Marine Optics. Elsevier, Amsterdam.

Jones, L.W., Kok, B., 1966. Photoinhibition of chloroplast reactions. Plant Physiology 41, 1037–1043.

Kirk, J.T.O., 1994. Light and photosynthesis in aquatic ecosystems, 2nd Edition. Cambridge University Press, Cambridge.

Nultsch, W., Agel, G., 1986. Fluence rate and wavelength dependence of photobleaching in the cyanobacterium *Anabaena variabilis*. Archives of Microbiology 144, 268–271.

Piazena, H., Häder, D.-P., 1994. Penetration of solar UV irradiation in coastal lagoons of the southern Baltic Sea and its effect on phytoplankton communities. Photochemistry and Photobiology 60, 463–469.

Piazena, H., Häder, D.-P., 1997. Penetration of solar UV and PAR into different waters of the Baltic Sea and remote sensing of phytoplankton. In: Häder, D.-P. (Ed.), The Effects of Ozone Depletion on Aquatic Ecosystems. Academic Press, R.G. Landes Company, Austin, pp. 45–96.

Seckmeyer, G., Mayer, B., Bernhard, G., 1998. The 1997 status of solar spectroradiometry in Germany: results from the national intercomparison of UV spectroradiometers. In: Seiler, W. (Ed.), Schriftenreihe des Fraunhofer-Institutes Atmosphärische Umweltforschung, Bd. 55, Garmisch-Partenkirchen.

Setlow, R.B., 1974. The wavelengths in sunlight effective in producing skin cancer: a theoretical analysis. Proceedings of the National Academy of Sciences of the United States of America: PNAS 71, 3363–3366.

Smith, R.C., 1989. Ozone, middle ultraviolet radiation and the aquatic environment. Photochemistry and Photobiology 50, 459–468.

Smith, R.C., Baker, K.S., 1978. Optical classification of natural waters. Limnology and Oceanography 23, 260–267.

Smith, R.C., Baker, K.S., 1981. Optical properties of the clearest natural waters (200–800 nm). Applied Optics 20, 177–184.

Tevini, M., Häder, D.-P., 1985. Allgemeine Photobiologie. Georg Thieme Verlag, Stuttgart, New York.

Vernet, M., Smith, R.C., 1997. Effects of ultraviolet radiation on the pelagic antarctic ecosystem. In: Häder, D.-P. (Ed.), The Effects of Ozone Depletion on Aquatic Ecosystems. Academic Press, R.G. Landes Company, Austin, pp. 247–265.

Voitek, M.A., 1990. Addressing the biological effects of decreasing ozone in the Antarctic environment. Ambio 19, 52–61.

Wängberg, S.-A., Selmer, J.-S., 1997. Studies of effects of UV-B radiation on aquatic ecosystems. In: Häder, D.-P. (Ed.), The Effects of Ozone Depletion on Aquatic Ecosystems. Academic Press, R.G. Landes Company, Austin, pp. 199–213.